RENDICONTI Società Italiana di Mineralogia e Petrologia, 36 (1), 1980: pp. 441-466

L. VILLARI *

THE ISLAND OF ALICUDI

ABSTRACT. — The island of Alicudi is the summit part of a huge volcanic structure extending widely below sea level, down to about 1100 m depth.

Eruptive products consist of pyroclastic layers, lawa flow and endogenous domes, forming a central strato-volcano which resulted from the activity of four subsequent volcanic cycles.

Volcanics are ranging in composition from basalts to high-K andesites and are characterized by a fast increase of K_2O content during differentiation. Major and trace element chemistry, in agreement with the mineralogy of the lavas, points out a magmatic affinity which is transitional between calc-alkaline and high-K calc-alkaline.

The potassium-type trace elements (Rb, Sr and Ba) show high concentration, which characterizes the Aeolian volcanism and is frequently reported with reference to island arc setting where high-K calc-alkaline to shoshonitic products occur.

Both the petrographic features and the chemical characters indicate that the Alicudi rock suite resulted from fractionation processes acting, at variance with the neighboring island of Filicudi, under relatively low pO_2 and high pH_2O.

The high concentration of K_2O, LEE and LILE, which is typical for the Aeolian Island magmatism, suggests that different degrees of partial melting may have affected a common source region giving rise to parent magmas further evolving under different conditions. Both melting and differentiation may account for the observed inter-island variations.

The cognate characters shown by the Aeolian volcanic products are in agreement with the evolution of the arc dynamics as suggested by BARBERI et al. (1973, 1974) and may reflect a relatively fractionated mantle source and/or a contribution of relevant elements from the subducted slab.

RIASSUNTO. — L'isola di Alicudi rappresenta la parte sommitale emersa di una struttura vulcanica di notevoli dimensioni che si sviluppa essenzialmente sotto il livello del mare, fino ad una profondità di circa 1.100 m.

I prodotti vulcanici affioranti sull'isola sono rappresentati da livelli piroclastici, colate laviche e cupole di ristagno che si susseguono a formare nel loro insieme uno strato-vulcano centrale. Tale edificio si è sviluppato nel corso dell'attività di quattro distinti cicli eruttivi.

Le vulcaniti studiate presentano una composizione compresa tra i basalti e le andesiti ricche in potassio e sono caratterizzate da un incremento particolarmente accentuato del contenuto in K_2O nel corso della differenziazione. La composizione chimica (elementi maggiori, in traccia e Terre Rare) e mineralogica delle lave indicano un'affinità magmatica di transizione tra calco-alcalina e calco-alcalina alta in potassio.

Gli elementi in traccia affini al potassio (Rb, Sr e Ba) mostrano le concentrazioni elevate che sono tipiche del vulcanismo Eoliano e che peraltro vengono comunemente descritte con riferimento alle strutture di arco insulare in cui affiorano rocce ricche in potassio o shoshonitiche.

Sia le caratteristiche petrografiche che quelle chimiche indicano coerentemente come la serie di differenziazione messa in evidnza ad Alicudi possa derivare da processi di frazionamento che, in contrasto con quanto osservato per la vicina isola di Filicudi, si sono realizzati in condizioni di bassa pressione parziale di O_2 ed alta pressione di H_2O.

Le elevate concentrazioni in K_2O, LREE e LILE osservate ad Alicudi — peraltro tipiche del magmatismo Eoliano — suggeriscono, in una visione più generale, come gradi diversi di fusione parziale di una sorgente comune possano aver dato luogo alla formazione di magmi

* Istituto Internazionale di Vulcanologia, V.le R. Margherita 6, Catania.

capostipiti che a loro volta abbiano subito processi evolutivi indipendenti, dominati da differenti condizioni di frazionamento. Le differenze rilevate tra i prodotti delle varie isole dell'arcipelago possono trovare spiegazione nella menzionata variabilità sia dei processi di fusione parziale che in quelli di frazionamento.

I caratteri di affinità messi in evidenza nell'ambito del vulcanismo delle Eolie, ben si accordano con la rapida evoluzione della dinamica dell'arco suggerita da BARBERI et al. (1973, 1974) e possono riflettere la natura relativamente frazionata di una sorgente posta nel Mantello e/o risentire dell'apporto degli elementi arricchiti (K_2O, Ba, Sr, ecc...) da parte dello « slab » in subduzione.

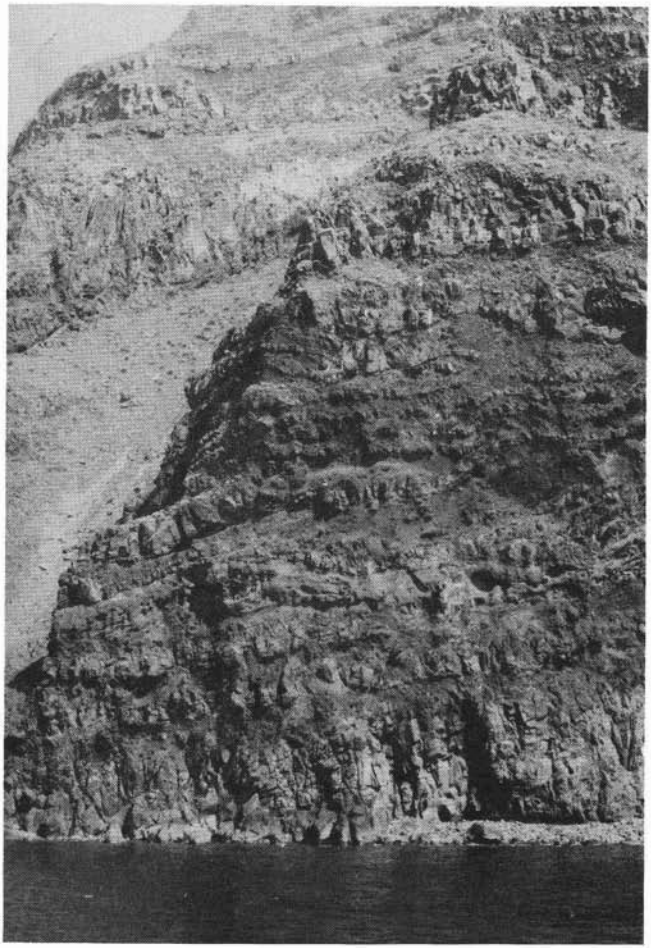

Fig. 1. — Island of Alicudi, western coast. The volcanic sequence attributed to the first cycle of activity on the island, mainly consists of thin lava flows with subordinate interbedded pyroclastic layers.

1. - Introduction

The island of Alicudi is the westernmost island of the Aeolian Archipelago, extending over about 5 km^2 and attaining a maximum elevation of 675 m a.s.l..

The island itself is the summit part of a huge volcanic structure widely extending below sea level, down to about 1100 m. The structure shows an approximately circular base and a well preserved conical shape, suggesting that the growth of the volcanic edifice occurred by mainly central eruptive activity giving rise to a steep strato-volcano with an average dip of about 20°. The whole strato-cone rises on a relative basement, formed by the surrounding sea floor, ranging between 1100 m and 1200 m depth. Besides the neighboring island of Filicudi, to the ENE, a well-shaped volcanic seamount rises from the same depth up to 590 m b.s.l., to the WNW (MORELLI, 1970).

Very few data were available up to now concerning the geology and the petrology of the island and they were contributed as part of more general papers on the Aeolian Archipelago (CORTESE and SABATINI, 1892; BERGEAT, 1918; KELLER, 1967; PICHLER, 1970; KLEIN et al., 1975). A geological survey was carried out by VILLARI and NAPPI in 1975 and the related geological map, printed in 1977, is folded in the back of this issue.

The present paper aims to contribute original data dealing with the volcanology, petrology and geochemistry of the island, which consists of basic and intermediate members of a calc-alkaline rock suite, in the framework of the Aeolian volcanism evolution.

2. - Geology

The island of Alicudi is exclusively made up by volcanic rocks, consiting of lava flows and domes and pyroclastic layers. The stratigraphical succession observed on the island allowed the distinction of four eruptive cycles which developed in a relatively continuous time sequence, as suggested by the lack of evidence for relevant erosional phases and/or formation of paleosoils. A well marked structural discontinuity can be observed between the first and the second cycle of activity. The latter developed after the formation of a large caldera, entirely filling the depression and overflowing the rim.

A large crater formed on top of the volcanic pile belonging to the second cycle of activity and later partially filled by domes and viscous lava flows attributed to the third cycle. Some of these lava flows overflowed the rim of the crater in its SE sector, running down the flank of the volcanic edifice down to the sea.

A late collapse of the summit dome during the fourth cycle gave rise to the outpouring of short tongues of viscous lava, associated with minor outflow from the southern flank.

During the whole eruptive sequence, no major migration of the main feeding conduit occurred and vents opened close to the main axis of the volcanic cone.

2.1. FIRST CYCLE: GALERA VOLCANIC COMPLEX

The best exposure of this early volcanic sequence can be observed along the western coast, in that section to the S of Sc. Galera. A pile of thin lava flows and

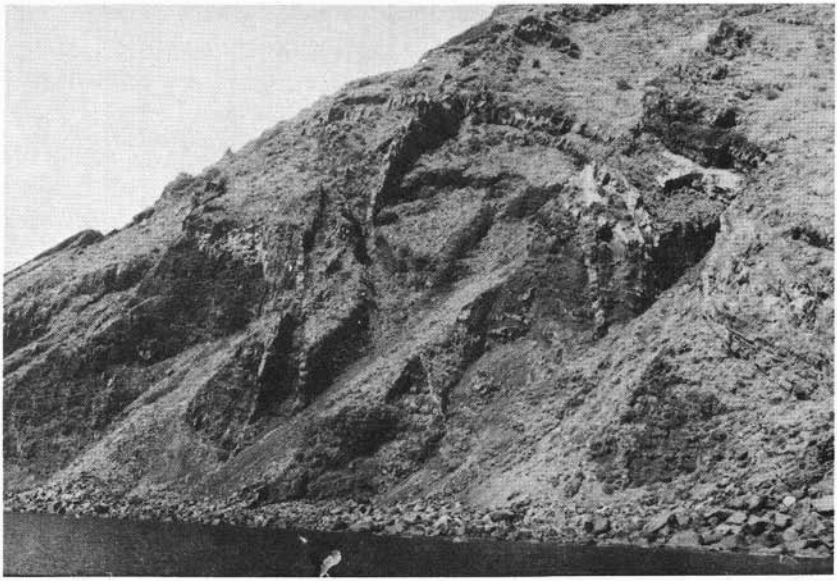

Fig. 2. — Island of Alicudi, western coast. A dense network of dikes and sills is injected into the volcanic pile, roughly trending according to a radial pattern.

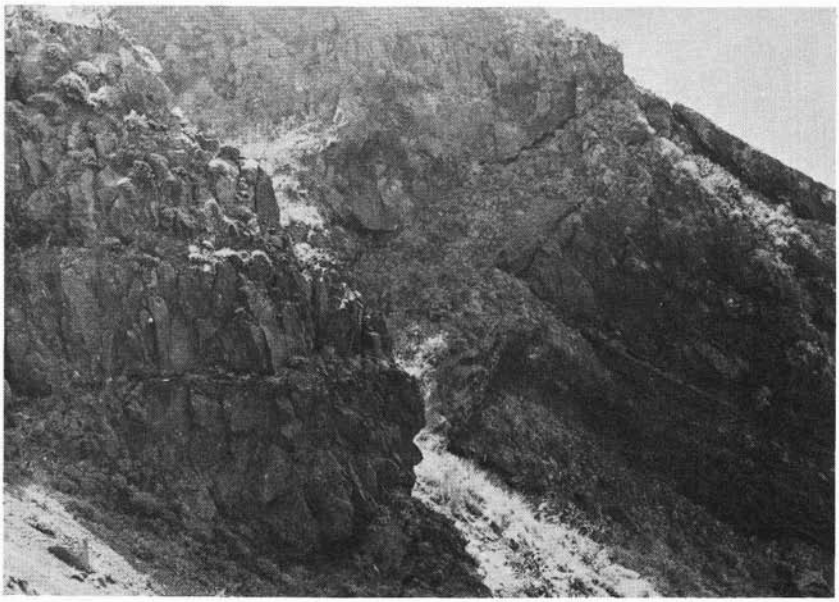

Fig. 3. — Island of Alicudi, south-western slope. The sharp angular unconformity between the volcanic units belonging to the Galera complex and the later lava flows filling the caldera depression is further emphasized by the quaquaversal layers mantling the rim of the caldera.

minor pyroclastic layers (fig. 1) is well exposed along the cliff and dissected by numerous deep canyons. A dense network of dikes and sills (fig. 2) can be observed

cutting through the series and roughly trending (dikes) towards the center of the volcanic structure, according to a radial pattern.

A well marked structural discontinuity occurs in this sector of the volcano, between 150 and 250 m altitude, where a sharp angular unconformity emphasizes the contact between the volcanic units belonging to the Galera complex and the overlying volcanic products, attributed to the second cycle of ativity on the island (fig. 3). The contact is characterized by the local occurrence of quaquaversal layers which develop at the top of the Galera volcanic sequence. The observed features, namely angular unconformity and quaquaversal structures, suggest that the exposed contact developed along the rim of a large volcanic depression, which is interpreted as the result of a caldera collapse occurring at the end of the first cycle of activity.

Lavas and pyroclastics belonging to the Galera complex outcrop along the northern coast and, in a minor exposure, along the northeast one. In spite of the angular unconformity which is still evident on the northern flank of the volcanic structure, no evidence has been observed that allows the caldera rim to be traced in that sector of the volcano. It is therefore inferred that the northern extension of the caldera rim developed to the north of the present shore-line.

The volcanic cycle on the whole is characterized by the prevalence of lava flows over pyroclastic products. The latter mainly consist of volcanic agglomerates and pyroclastic flows, with minor interbedded fall and surge deposits. Facies examination of pyroclastics points out the close proximity of the vent area, suggesting that the emplacement of the eruptive units occurred along the flank of a steep volcanic structure. Lava flows show a thickness rarely exceeding a few meters and a well developed scoriaceous crust forming the uppermost part of each single flow unit. Hand specimen examination revealed the constant presence of olivine and pyroxene phenocrysts in a fine-grained groundmass. Very often, even the more dense portion of lava flows, are finely vesiculated.

2.2. Second cycle: Dirituso volcanic complex

The volcanic sequence which was ascribed to the second cycle of activity on the island is characterized by the prevalence of pyroclastic materials over lava flows. Volcanics belonging to this cycle outcrop over about one half of the island and are well exposed mainly on the northern and western sector. On the upper slopes of the western flank they unconformably rest on the volcanic units of the Galera complex (fig. 4), filling the caldera depression which formed at the end of the first cycle. In this area the average dip of Dirituso volcanic units gradually changes proceeding upward in the stratigraphic section. The basal units are clearly dipping inland while lava flows and pyroclastic layers dip towards the sea in the uppermost portion of the sequence. Proceeding northward they entirely cover the flank of the volcano, reaching the sea near P. di Malopasso.

On the northern slope of the volcanic structure the contact between the Dirituso volcanics and the underlying Galera complex develops at about 350 m altitude, showing a clear unconformity between the two volcanic piles.

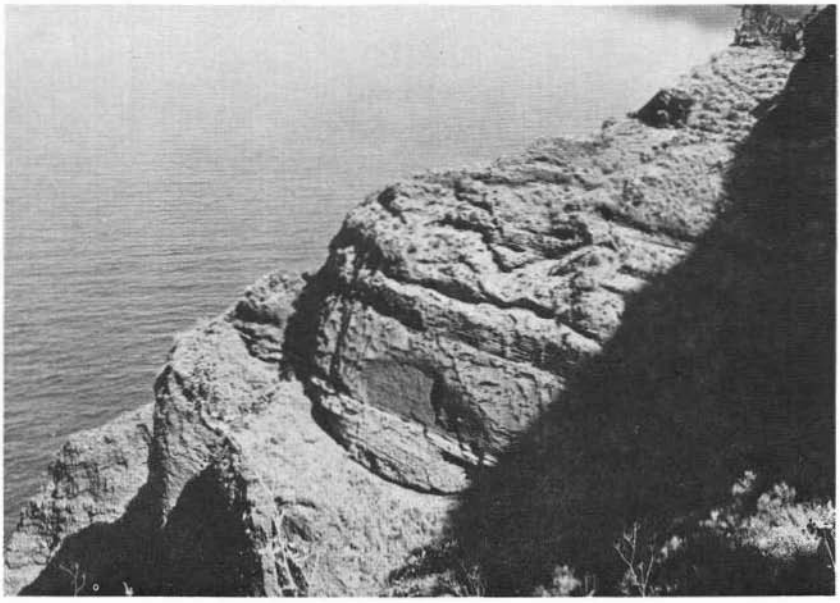

Fig. 4. — Island of Alicudi, western slope. Volcanics from the second cycle of activity mainly consist of pyroclastic layers, unconformably resting on the Galera complex (lower left corner).

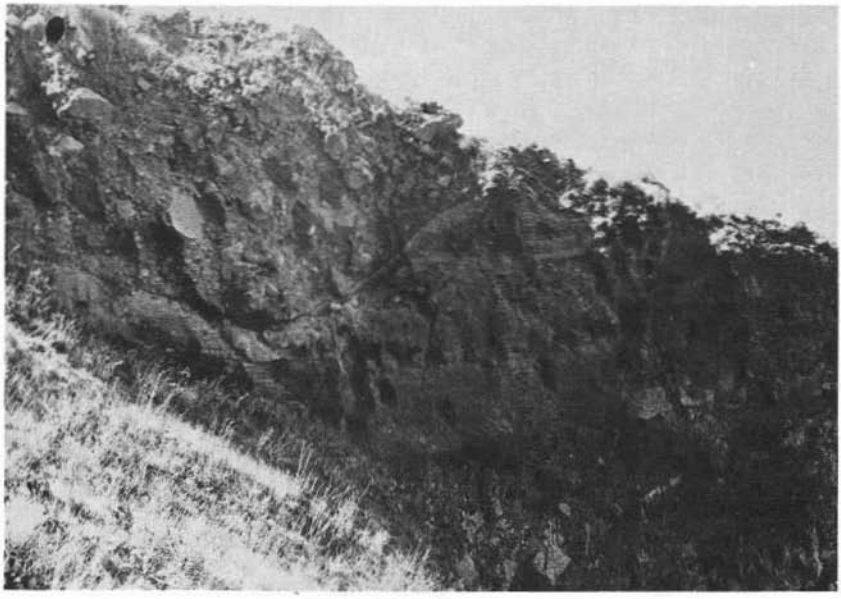

Fig. 5. — Island of Alicudi, eastern slope. In a closer proximity of the vent area the pyroclastic products of the second cycle show the local occurrence of lahar type deposits.

The older Galera volcanics are almost entirely obscured in the eastern sector where the volcanic products of the second cycle attain the sea-shore. On the upper

slope of the eastern flank volcanic agglomerates and breccias (fig. 5) widely outcrop, pointing out the close proximity of the vent area. A crater rim is in fact clearly exposed in the northern and eastern summit area and partly obliterated in its south-eastern sector by the emplacement of the subsequent lava flows and domes belonging

Fig. 6. — Island of Alicudi, northern coast. The second cycle of activity is dominated by pyroclastics, among which pyroclastic flows often occur. Dikes are injected in the sequence and well exposed along the cliff.

to the third phase of activity on the island. The deep erosion which affected the western slope of the volcano prevents the crater rim from being traced in the field, but the inferred developement in that sector indicates that a crater of about 1 km in diameter was established on top of the Dirituso volcanic pile. The crater depression was later filled with viscous lava flows and domes during the third cycle of activity, with the exception of an area of limited extent, close to the northern edge of the crater. In this area the crater floor is covered by a thick layer of reworked volcanoclastic material.

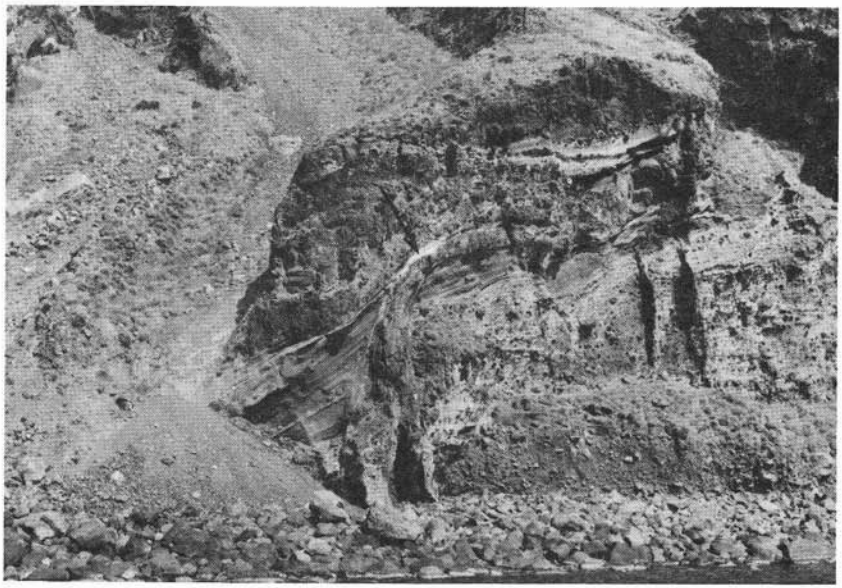

Fig. 7. — Island of Alicudi, north-western coast. Pyroclastic flows are locally interbedded with fall and surge deposits of the second cycle. The arrow indicates a dike grading into a sill.

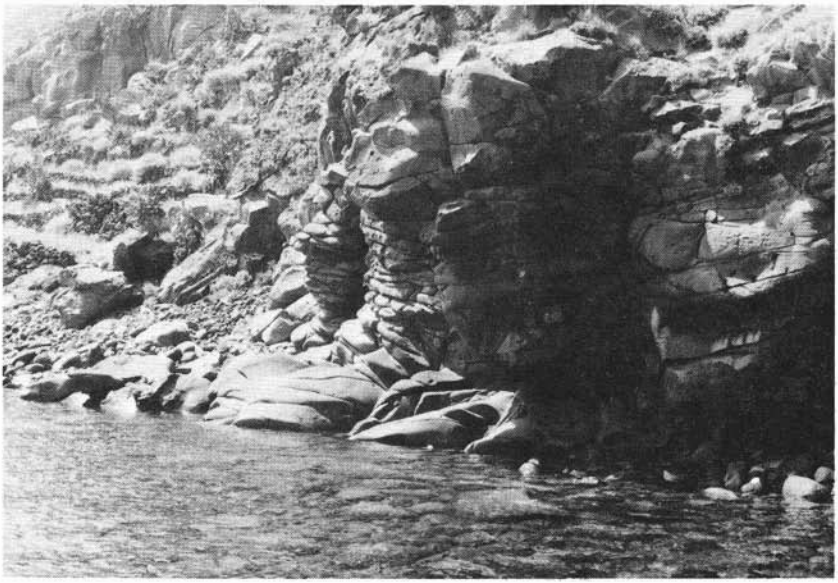

Fig. 8. — Island of Alicudi, south-eastern coast. A viscous lava flow belonging to the third cycle of activity shows well-developed lamination structures in a section along the sea-cliff.

A minor outcrop of the Dirituso volcanics can be also observed along the lower southwestern slope. Volcanic products attributed to the second cycle are exposed on

the sea-cliff and can be traced upslope to approximately 100 m altitude, progressively disappearing beneath younger lava flows.

The whole sequence is cut by numerous dikes and sills (figs 6 and 7), which are better exposed on the western and northern sectors, as previously observed for th older Galera volcanics. The local abundance of intrusions, which are regarded as the feeding structures of the central volcanic activity, is considered to be the mere consequence of a more efficient erosion, which developed in that area because of the sea action, in view of the prevailing westerly winds. Erosive processes, cutting deep into the volcanic structure, allowed the innermost part of the volcanic edifice to become exposed.

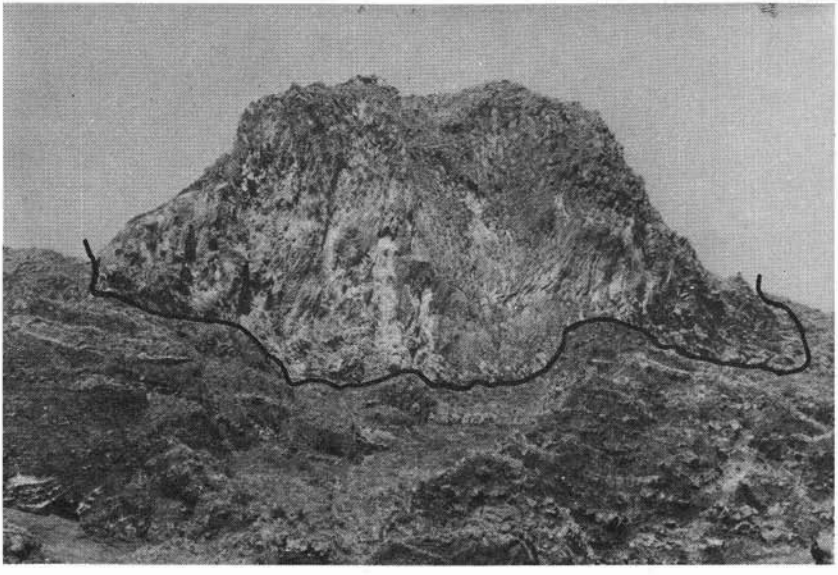

Fig. 9. — Island of Alicudi, south-western upper slope. An endogenous dome belonging to the third cycle shows evident laminar structures in its innermost part, while the outer carapace is characterized by a blocky surface.

The pyroclastic products, which are dominant in the volcanic pile, mainly consist of pyroclastic flows (fig. 6) and minor fall and surge deposits (fig. 7). Volcanic agglomerates and vent opening breccias are locally observed. Flow direction and facies distribution of the pyroclastic surges point to a radial distribution, relative to the main strato-cone. No evidence has been observed suggesting the activity from parasitic vents on the flanks of the main structure.

Lava flows are interbedded with the pyroclastic layers and they show a wide range in thickness, suggesting a variable viscosity of the erupted magma. An overall increase in thickness is however noticed proceeding upward in the stratigraphic sequence. The scoriaceous crust of lava flows is well developed, both on top and the base of thinner units, while it is pratically absent in those units showing a greater thickness.

Olivine and pyroxene phenocrysts are observed on hand specimens throughout the sequence and they are associated with plagioclase phenocrysts in the more viscous lava flows.

2.3. Third cycle: Montagna volcanic complex

The third cycle of activity consists, almost exclusively, of lava flow and domes which developed on the summit area and on the southeastern slope of the volcano. Lava flows reached the sea mainly in that section of the coast near Perciato, where the thick flow units are well exposed showing a definite lamination structure (fig. 8). A few lava tongues also attained the sea-shore farther to the west, flowing in a radial gully which marks the contact between the Galera and Dirituso complexes.

Dome structures are well exposed in the summit area (fig. 9), mostly filling the crater depression which is cut into the Dirituso volcanics. The viscous lava which erupted on the crater floor, progressively grew and accumulated, exceeding the morphological capacity of the crater itself. Thick lava tongues overflowed the southeastern sector of the crater rim, expanding downslope on the flank of the volcanic edifice. In spite of their high viscosity, lavas were able to flow on the flank of the volcano, due to the steep slope of the structure. A closer examination of the domes reveals their endogenous character. Flow lamination structures are largely developed in the innermost parts of the domes, while the outer carapace is characterized by a blocky surface (fig. 9).

The dome which extruded at the very top of the volcanic pile appears to have suffered a summit collapse, giving rise to the formation of an elliptical crater. The major axis of the depression is trending in a NW direction, coherently with the strike of a fault system which dissects the whole strato-volcano.

Hand specimens both of domes and lava flows reveal the occurrence of plagioclase and pyroxene phenocrysts, in a finegrained to glassy groundmass. Rare olivine phenocrysts are also observed.

2.4. Fourth cycle: Filo dell'Arpa volcanic complex

The late stage of volcanic activity on the island gave rise to the eruption of limited volumes of lava, forming short and thick flows mainly on the southern slope of the volcano. Only a minor tongue of these flows attained the sea, showing a front of about a few tens of meters in breadth. Some of the lava flows seems to originate from the upper slope of the volcanic structure, but no further evidence has been observed that allows a more precise location of the related vents. Two lava flows originate, on the contrary, from a well defined fracture running across the collapsed crater on the summit dome, according to its main axis. The distribution of both the observed and the inferred vents probably suggests a structural control on vent location, due to the already-mentioned fault system trending in a NW-SE direction.

As far as the phenocryst occurrence is concerned, the lavas belonging to this late stage of volcanism on the island, are very similar to those of the previous cycle. Plagioclase is the dominant phenocryst phase, associated with minor but ubiquitous pyroxene.

3. - Petrology

The sample collection carried out during the geological mapping of the island in 1975 allowed a careful examination of the petrological characters of this rock suite. Thin section observations on all the sampled rock specimens (53) suggested the selection of 24 representative lavas, on which major and trace element analyses were carried out (Tables 1 and 2). REE were also determined on 6 samples (Table 3).

Very little data were available, before the present study, concerning the petrography (Bergeat, 1918) and the geochemistry (Klein et al., 1975) of this rock suite, there not being any precise reference to the stratigraphic position of the analyzed samples.

The whole rock association outcropping on the island of Alicudi defines a subalkaline sequence showing transitional characters between calc-alkaline and high-K calc-alkaline. The sequence concerned consists of basalts - basaltic andesites - -high-K andesites, according to the classification proposed by Peccerillo and Taylor (1976). Basalts and basaltic andesites are the dominant members of the suite, while high-K andesites are confined to the more recent domes and lava flows of the third and fourth cycle of activity.

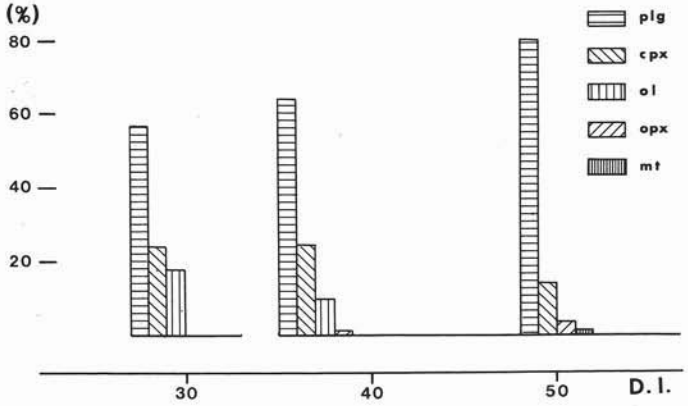

Fig. 10. — Island of Alicudi. Persistence and relative abundance (%) of phenocrysts in the Alicudi rock suite, as a function on the Differentiation Index of Thornton and Tuttle (1960).

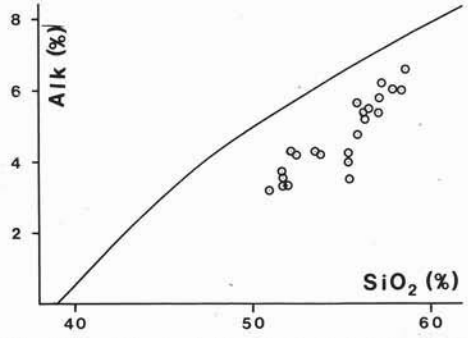

Fig. 11. — Island of Alicudi. $Na_2O + K_2O$ (Alk) vs. SiO_2 plot for the analysed lava samples. The boundary line between the alkaline and the subalkaline fields is traced after Irvine and Baragar (1972).

3.1. Petrography

Basalts show a porphyritic texture, which is characterized by large proportions of phenocrysts, ranging from 40 % to 50 % of the total rock. The groundmass largely consists of microlites of the same minerals which occur as phenocrysts, associated with finely dispersed opaque minerals. Interstitial glass is

TABLE 1

Major elements of Alicudi volcanics (Aeolian Islands)

	GALERA VOLCANIC COMPLEX					DIRITUSO VOLCANIC COMPLEX		
	Al 13*	Al 11*	Al 25*	Al 24*	Al 23*	Al 27*	Al 04	Al 02
SiO_2	50.97	51.58	55.35	55.41	55.43	51.73	51.85	52.25
TiO_2	.83	.69	.72	.72	.71	.80	.66	.62
Al_2O_3	16.79	16.57	16.50	16.89	16.91	16.61	14.40	18.51
Fe_2O_3	6.34	5.95	4.78	3.63	5.31	5.77	4.03	4.12
FeO	2.73	1.72	2.37	3.30	1.80	3.01	4.74	3.44
MnO	.18	.16	.14	.16	.16	.18	.12	.12
MgO	6.89	7.64	6.28	6.18	5.94	6.75	9.87	5.34
CaO	11.05	10.45	9.02	8.67	8.71	10.54	9.81	8.55
Na_2O	2.22	2.76	2.20	2.54	2.84	2.64	2.30	2.80
K_2O	.90	1.01	1.32	1.38	1.41	.89	1.02	1.52
P_2O_5	.30	.33	.34	.32	.33	.42	.17	.23
H_2O^-	–	–	–	–	–	–	–	.62
L.O.I.	.81	1.14	.99	.80	.45	.65	1.26	1.15
	100.01	100.00	100.01	100.00	100.00	99.99	100.22	99.47
$Mg/Mg+Fe^{2+}$	.62	.69	.66	.66	.66	.62	.70	.60
				CIPW-NORM				
Q	5.78	3.12	12.23	9.73	9.50	5.57	1.94	5.34
or	5.32	5.97	7.80	8.15	8.33	5.26	6.03	8.98
ab	18.78	23.34	18.61	21.48	24.02	22.33	19.46	23.68
an	33.19	29.84	31.25	30.61	29.23	30.85	25.96	33.45
di	15.30	15.44	8.77	8.13	9.20	14.58	17.11	5.88
hy	10.06	11.86	11.57	13.72	10.52	10.06	21.00	12.31
mt	6.98	4.07	6.01	5.26	4.27	7.97	5.84	5.97
il	1.58	1.31	1.37	1.37	1.35	1.52	1.23	1.56
ti	–	–	–	–	–	–	–	–
ap	.71	.78	.81	.76	.78	1.00	.40	.55
he	1.53	3.15	–	–	–	.27	–	–
D.I.	30	32	39	39	42	33	27	38

* X Ray Spectromety, with the exception of H_2O, FeO, MgO (AA) and Na_2O (FF). All the other analyses by chemical wet methods. Analyses by: M. CARÀ and F. TURCHIO (wet method), N. BRUNO and A. PELLEGRINO (XRF).

always present in variable proportions. Rare glomerphiric aggregates of olivine and pyroxene were also observed in some samples.

Plagioclase is the predominant phenocryst phase, representing 45 % to 65 % of of the total phenocrists. Most of the crystals show normal zoning with superimposed weaker oscillatory zoning. Frequent glass inclusions are observed in phenocrysts. The An content of larger phenocrysts ranges between 70 % and 75 %, while smaller phenocrysts and groundmass microlites are usually An_{60} to An_{70} in composition.

Clinopyroxene represents 15 % to 35 % of phenocrysts and its optical properties ($2V\gamma$ 54°-58°; $c\wedge\gamma$ 40°-45°) are those for augite.

Subhedral to rounded olivine grains are present in fairly large proportions,

TABLE 1: continued

	DIRITUSO : continue			MONTAGNA VOLCANIC COMPLEX				
	Al 03	Al 22	Al 06	Al 07	Al 011	Al 1	Al 09	Al 012
SiO_2	52.40	53.46	53.75	53.52	55.77	56.87	56.20	56.27
TiO_2	.82	.57	.77	.77	.72	.80	.85	.70
Al_2O_3	17.90	16.33	15.56	15.56	17.52	17.59	17.35	17.33
Fe_2O_3	5.04	3.98	6.07	3.55	3.82	4.84	4.34	5.24
FeO	2.87	2.01	1.94	4.21	2.87	2.72	2.72	1.79
MnO	.10	.13	.12	.13	.12	.14	.13	.12
MgO	5.74	10.91	7.56	7.56	4.83	4.13	4.83	5.04
CaO	9.53	7.39	9.39	9.39	6.72	7.57	6.73	7.29
Na_2O	2.76	2.86	2.74	2.76	3.58	3.20	3.36	3.20
K_2O	1.42	1.71	1.48	1.54	2.08	1.60	2.02	2.02
P_2O_5	.25	.32	.35	.35	.42	.26	.40	.46
H_2O^-	-	-	-	-	.44	.20	.43	.10
L.O.I.	1.39	.32	.63	.97	1.35	.59	.92	.34
	100.22	99.99	100.36	100.31	100.24	99.51	100.28	99.89
$Mg/Mg+Fe^{2+}$	.61	.80	.67	.67	.61	.54	.60	.61
				CIPW-NORM				
q	5.55	.82	5.77	3.53	7.15	11.01	9.31	9.44
or	8.39	10.10	8.74	9.10	12.29	9.45	11.93	11.93
ab	23.34	24.19	23.17	23.34	30.28	27.06	28.42	27.06
an	32.26	26.67	25.79	25.52	25.60	28.91	26.30	26.96
di	10.41	6.14	14.40	14.89	3.92	5.40	3.49	4.87
hy	9.46	24.31	12.15	15.54	11.33	7.78	10.65	10.29
mt	7.20	5.25	4.41	5.15	5.54	6.90	6.29	4.13
il	1.56	1.08	1.46	1.46	1.37	1.52	1.61	1.33
ti	-	-	-	-	-	-	-	-
ap	.59	.76	.83	.83	1.00	.62	.95	1.07
he	.07	-	-	-	-	-	-	2.39
D.I.	37	35	38	36	50	48	50	48

ranging from 15 % to 25 % of phenocrysts. Some of the olivine crystals are deeply affected by alteration which, proceeding through cleavage and fracture planes, causes the progressive transformation into serpentine. The composition of fresh phenocrysts was estimated, according to their optical properties ($2V\gamma$ 50°-92°), about Fa_{15-20}. Small olivine grains were also observed in the groundmass.

Fe-Ti oxides are generally not represented among phenocryst phases, except in sample Al 11 where they form less than 1 % of phenocrysts.

Basaltic andesites are porphyritic in texture and similar to the basalts described above. The phenocryst content ranges from 35 % to 55 % of the whole rock and it is characterized by a large proportion of plagioclase relative to the ferromagnesian minerals. The groundmass mainly consists of opaque minerals, plagioclase and pyroxene microlites, with minor glass and rare olivine grains. Subangular to rounded interlocking aggregates, mainly consisting of plagioclase with minor pyroxene and olivine, are frequently observed.

TABLE 1: continued

	MONTAGNA : continue				FILO DELL'ARPA VOLCANIC COMPLEX	
	Al 08	Al 4*	Al 01	Al 18*	Al 010	Al 013
SiO_2	57.12	57.25	57.90	58.59	56.50	58.40
TiO_2	.62	.69	.60	.60	.77	.65
Al_2O_3	17.10	17.05	17.20	18.21	17.39	17.97
Fe_2O_3	4.60	4.34	4.08	3.34	4.38	5.95
FeO	2.29	1.94	2.58	2.37	2.36	.43
MnO	.12	.15	.11	.13	.12	.08
MgO	4.63	4.24	4.03	2.83	4.83	3.12
CaO	7.29	7.24	6.17	6.24	6.72	6.73
Na_2O	3.42	3.90	3.78	4.19	3.42	3.58
K_2O	1.99	2.27	2.24	2.45	2.08	2.32
P_2O_5	.42	.46	.37	.43	.42	.45
H_2O^-	.14	-	.14	-	.87	-
L.O.I.	.25	.47	.46	.43	.62	.45
	100.19	100.00	99.86	100.00	100.48	100.32
$Mg/Mg+Fe^{2+}$	.59	.59	.57	.52	.61	.52
				CIPW-NORM		
q	10.02	7.65	10.11	9.27	9.26	11.86
or	11.76	13.41	13.23	14.48	12.29	13.71
ab	28.93	32.98	31.97	35.35	28.93	30.28
an	25.44	22.32	23.35	23.70	25.96	26.09
di	6.21	8.24	3.77	3.49	3.60	2.63
hy	8.65	6.73	8.53	5.93	10.35	6.55
mt	5.40	4.74	5.92	4.84	5.77	-
il	1.56	1.31	1.52	1.52	1.46	1.08
ti	-	-	-	-	-	.69
ap	1.00	1.09	.88	1.02	1.00	1.07
he	.88	1.07	-	-	.40	5.95
D.I.	51	54	55	59	50	56

Plagioclase is by far the most abundant phenocryst phase, ranging between 60 % and 80 % of the total phenocrysts. The An content of phenocrysts is normally comprised between 55 % and 65 %, but more calcic cores up to An_{75} were observed in some large crystals. Microlite composition is always in the range shown by the outer rim of phenocrysts (An_{55-60}).

Clinopyroxene represents 15 % to 35 % of the phenocrysts, showing the same optical characters as in basalts.

Orthopyroxene occurs as phenocryst in most of the samples, ranging from 1 % to 4 % of the total phenocrysts. The composition deduced from the observed optical characters ($2V\alpha$ 70°-75°), is En_{80-85}.

Olivine content is highly variable (1 % to 18 %) and normally decreases with increasing SiO_2. Most of the olivine grains are intensely resorbed and almost entirely transformed into alteration products of the serpentine group. Some fresh crystals have however been observed, showing a composition of Fa_{15-20}.

Fe-Ti oxides are finely dispersed into the matrix and they do not occur as phenocrysts.

High-K andesites are mainly porphyritic in texture and contain variable amounts of phenocrysts, ranging from 35 % to 50 % of the total rock. They are characterized by the almost total lack of olivine and by the appearance of Fe-Ti oxides among

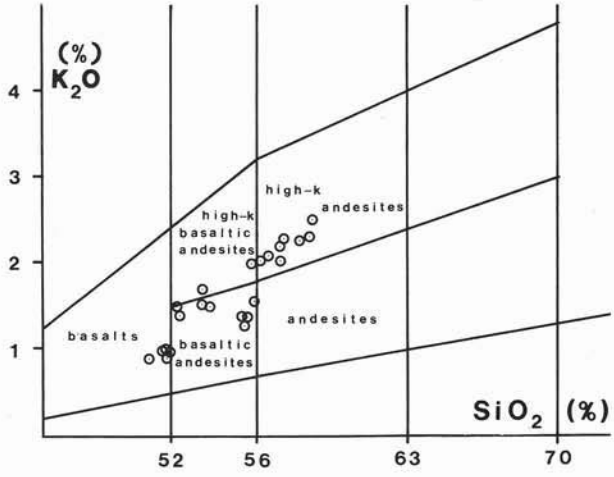

Fig. 12. — Island of Alicudi. K_2O vs. SiO_2 plot for the analysed samples. The classification scheme proposed by PECCERILLO and TAYLOR (1976) is reported.

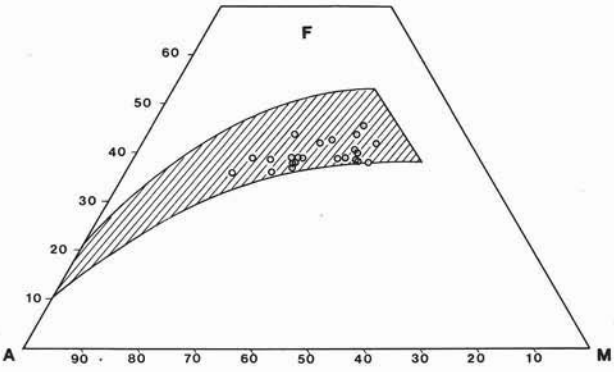

Fig. 13. — Island of Alicudi. The AFM diagram shows that the Alicudi rock suite is characterized by a weak iron enrichment. The shaded area represents the field of calc-alkaline suites after RINGWOOD (1974).

the phenocrysts. The groundmass consists of opaque minerals, pyroxene and plagioclase microlites, associated with variable percentage of glass. Trachytic textures have been observed in samples from domes and viscous lava flows.

Plagioclase (70 % to 85 % of total phenocrysts) ranges in composition between An_{55} and An_{65}. Calcic cores (An_{75}) are very common in larger phenocrysts, and the apparent gap in composition between cores and outer rims suggests that the

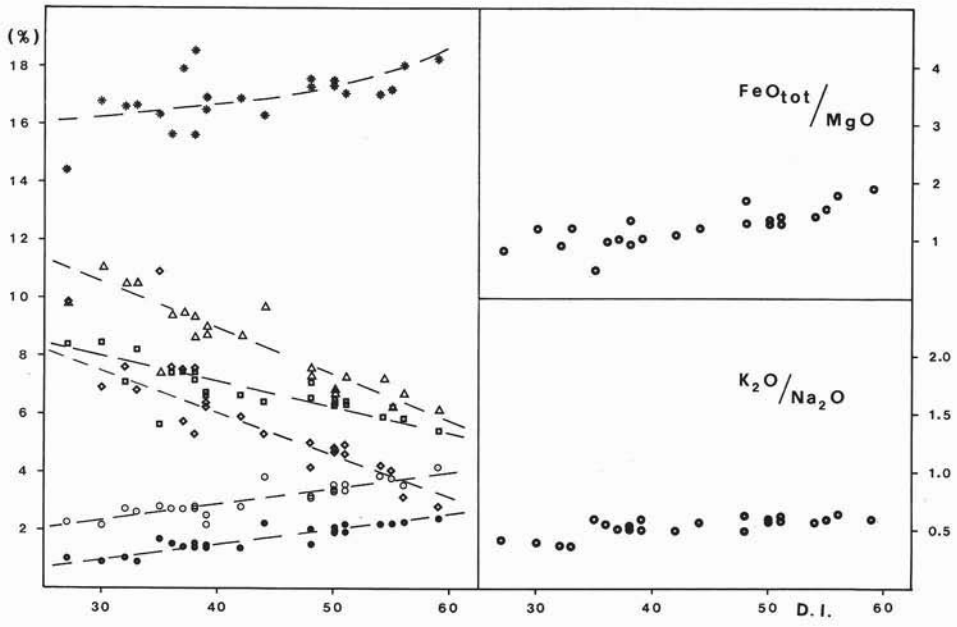

Fig. 14. — Island of Alicudi. Variation diagram of major oxides vs. Differentiation Index. *, Al_2O_3; □, $FeO_{tot.}$; △, CaO; ◇, MgO; ○, Na_2O; ●, K_2O. The variation of $FeO_{tot.}/MgO$ and K_2O/Na_2O ratios is also shown on the right.

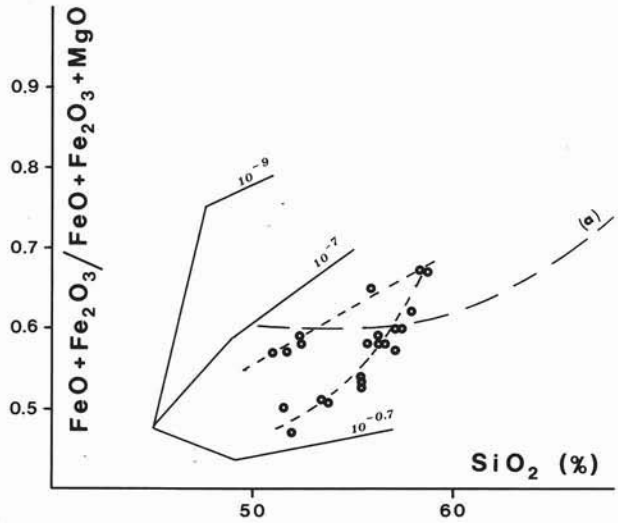

Fig. 15. — Island of Alicudi. The iron/magnesium ratio vs. SiO_2 plot for the Alicudi volcanics defines two different trends of iron enrichment. In the diagram are also reported the experimental curves obtained by the fractional crystallization of liquids under constant pO_2 of $10^{-0.7}$, 10^{-7}, 10^{-9} atm respectively, in a system MgO + FeO + Fe_2O_3 + $CaAl_2Si_2O_8$ + SiO_2 (HAMILTON and ANDERSON, 1967). The dashed line (*a*) represents the differentiation trend for a typical calc-alkaline suite, i.e. the Cascade Range.

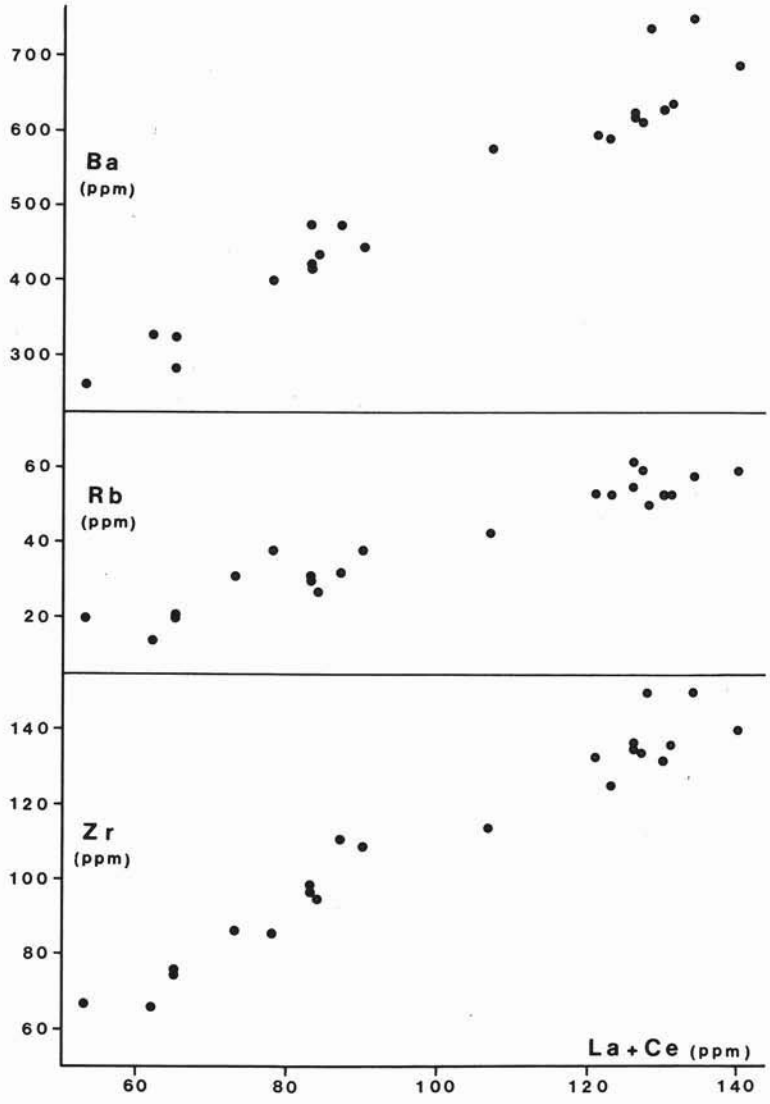

Fig. 16. — Island of Alicudi. The variation of Ba, Rb and Zr vs. La + Ce shows a positive linear correlation, suggesting a comagmatic affinity for the Alicudi rock suite.

former are relicts from a more basic magma. Microlites show the same composition of phenocryst rims.

Clinopyroxene (10 % to 20 %) and orthopyroxene (1 % to 7 %) phenocrysts show the same optical characteristics as observed in basaltic andesites. They can be classified as augite and bronzite respectively.

Olivine phenocrysts are constantly less than 1 % of all the phenocrysts and totally lacking in some samples. No olivine occurs in the groundmass.

Fe-Ti oxides represent 1 % to 2 % of the phenocrysts.

The persistence and relative abundance of phenocrysts throughout the rock suite are summarized in fig. 10.

3.2. Major elements

The Alicudi rock suite defines a subalkaline trend (fig. 11) consisting of basic to intermediate members which alternate in the stratigraphic sequence. An overall increase in SiO_2 content is nevertheless observed with time, i.e. the most recent eruptions gave rise to the outflow of lavas consistently spanning in a narrow SiO_2

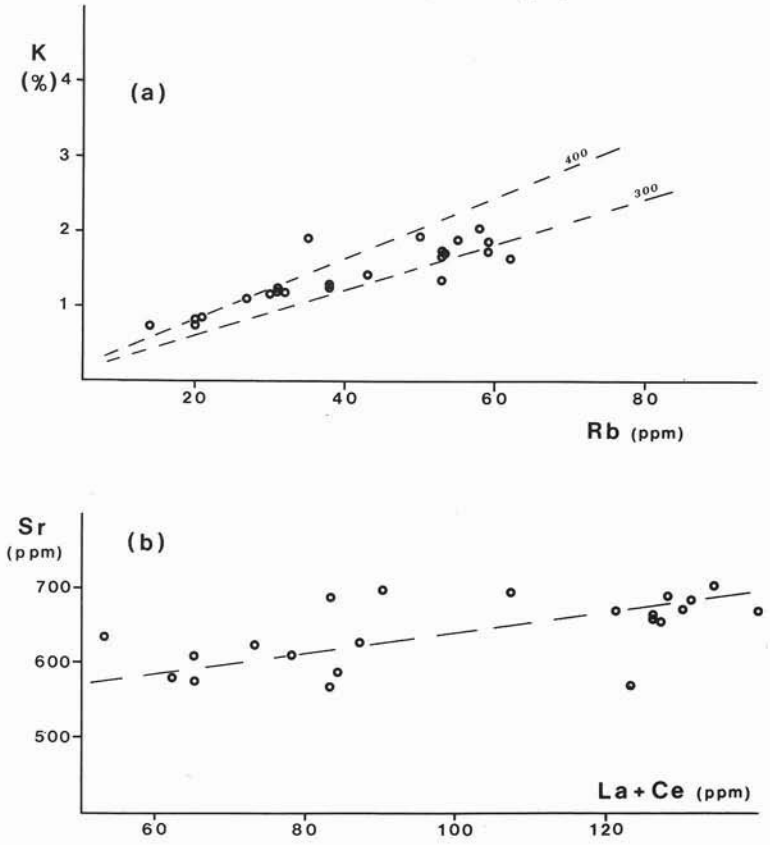

Fig. 17. — Island of Alicudi. K vs. Rb plots of Alicudi samples (*a*) show a decrease of K/Rb ratio as fractionation proceeds. The overall increase of Sr (*b*) during differentiation suggests a minor role of plagioclase in fractionation.

range (56 %-58 %); more basic rocks are virtually lacking.

The classification of the analyzed samples (Table 1) was obtained according to the K_2O vs. SiO_2 plot (fig. 12), after the scheme proposed by Peccerillo and Taylor (1976). Basalts and basaltic andesites are the dominant members of the first and second cycles of activity, whole high-K andesites prevail in the later cycles. It is to be noted, however, that an apparent deviation from a well defined trend affects samples in the basaltic andesites field. A small group plots (4 samples) shows a definitely

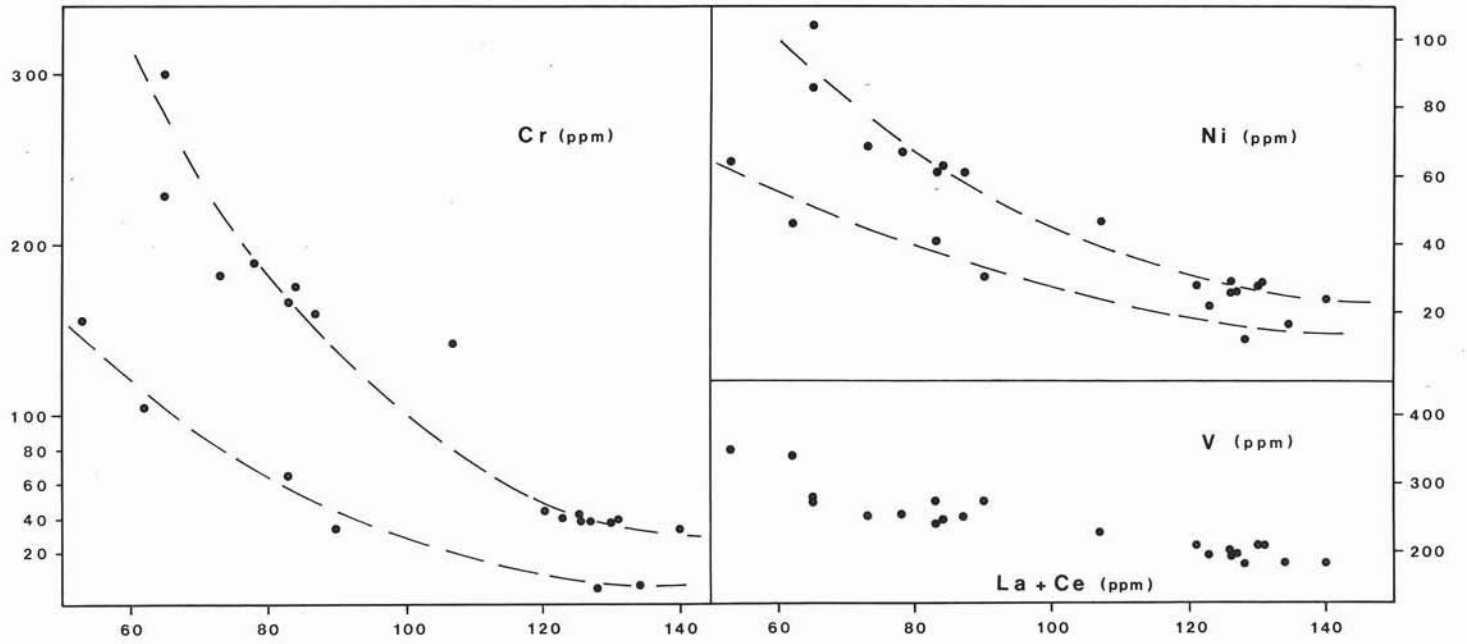

Fig. 18. — Island of Alicudi. Cr, Ni and V vs. La + Ce plots for the Alicudi volcanics. Ni and Cr distribution both define the occurrence of two different trends showing similar patterns. A peculiar features of the Alicudi rocks is the high Ni and Cr abundance in most of the basalts and basaltic andesites. Concentrations up to 300 ppm and 100 ppm are observed for Cr and Ni respectively on the basaltic end members of the upper trend.

TABLE 2

*Trace element analyses of Alicudi volcanics (Aeolian Islands)**

	Al 04	Al 13	Al 11	Al 27	Al 22	Al 07	Al 03	Al 06	Al 02	Al 25	Al 24
La	25	19	24	24	42	30	29	25	35	32	30
Zr	75	67	76	66	114	86	99	87	109	95	97
Ba	282	262	342	328	579	399	420	417	445	435	476
Rb	21	20	20	14	43	38	31	31	38	27	30
Sr	575	635	611	579	694	611	688	624	697	588	569
Cr	298	158	229	105	143	190	65	183	34	176	167
Ni	104	64	86	46	47	67	41	69	31	63	61
V	276	350	280	341	230	254	277	256	276	248	241
Y	26	25	27	10	20	19	30	23	31	20	16
Nb	17	10	11	13	15	9	12	10	14	12	13
K/Rb	405	375	420	529	330	337	381	397	331	407	383
Rb/Sr	.04	.03	.03	.02	.06	.06	.05	.05	.05	.05	.05
Ba/Rb	13.43	13.10	17.10	23.43	13.47	10.50	13.55	13.45	11.71	16.11	15.87
Ba/Sr	.49	.41	.56	.57	.83	.65	.61	.67	.64	.74	.84
Cr/V	1.08	.45	.82	.31	.62	.75	.23	.71	.12	.71	.69
V/Ni	2.65	5.47	3.26	7.41	4.89	3.79	6.76	3.71	8.90	3.94	3.95
Nb/Y	.65	.40	.41	1.30	.75	.47	.40	.43	.45	.60	.81

	AL 23	Al 1	Al 012	Al 09	Al 010	Al 011	Al 08	Al 4	Al 01	Al 013	Al 18
La	34	50	47	49	48	47	48	50	53	49	51
Zr	111	132	133	125	134	138	136	135	140	150	150
Ba	475	628	596	591	612	619	634	620	685	739	750
Rb	32	53	53	53	59	62	53	55	59	50	58
Sr	631	673	670	568	660	655	687	666	670	689	703
Cr	160	38	44	41	39	39	40	43	34	10	11
Ni	61	28	28	22	26	26	29	29	24	12	17
V	253	210	213	197	197	194	210	201	185	183	189
Y	21	29	28	23	26	24	23	21	24	40	25
Nb	20	20	23	17	18	20	20	21	21	30	31
K/Rb	366	251	317	317	293	279	311	344	315	386	350
Rb/Sr	.05	.08	.08	.09	.09	.09	.08	.08	.09	.07	.08
Ba/Rb	14.84	11.85	11.25	11.15	10.37	9.98	11.96	11.27	11.61	14.78	12.93
Ba/Sr	.75	.93	.89	1.04	.93	.95	.92	.93	1.02	1.07	1.07
Cr/V	.63	.18	.21	.21	.20	.20	.19	.21	.18	.05	.06
V/Ni	4.15	7.50	7.61	8.95	7.58	7.64	7.24	6.93	7.71	15.25	11.12
Nb/Y	.95	.69	.82	.74	.69	.83	.87	1.0	.88	.75	1.24

* XRF analyses by G. CRISCI, University of Calabria, Cosenza (Italy).

lower K_2O concentration, clustering close to the boundary line between basaltic andesite and andesite fields. The regression line fitting most of the samples shows a steeper slope, if compared with the boundary line between calc-alkaline and high-K calc-alkaline fields, showing a marked K_2O enrichment through the rock suite.

AFM plots of Alicudi samples (fig. 13) show a weak iron enrichment, even in the less differentiatiated members. Plots are consistently within the field defined by RINGWOOD (1974) for the calc-alkaline rock suites, showing a flat trend which is typical of most orogenic associations.

The variation diagram (fig. 14) of major oxides vs. D.I. (THORNTON and TUTTLE, 1960) shows a steady increase of Na_2O and K_2O with increasing D.I., while FeO_{tot}, CaO and MgO progressively decrease. Al_2O_3 content is comprised between 15 % and 18 % and it is characterized by an overall increase with increasing D.I.. The $FeO_{tot.}/MgO$ ratio is constantly below 2, with very few exceptions among the more differentiated lavas (samples Al 18 = 2.04), suggesting a magmatic affinity similar to island arc volcanics (JAKES and WHITE, 1972). The K_2O/Na_2O ratio is approximately constant throughout the whole series, ranging between 0.5 and 0.6. Such a feature is coherent with the character stressed by the iron/magnesium ratio and confirms the island arc magmatic affinity of Alicudi volcanics (JAKES and WHITE, 1972). TiO_2, CaO and Na_2O abundances also show values which are in good agreement with the average concentration reported by EWART (1976) for the island arc suites and considered to be consistently different from that of their continental margin compositional equivalent.

In spite of some scattering in the referred diagrams, the overall coherence of sample distribution according to a defined trend suggests a possible comagmatic affinity for the rocks forming the Alicudi suite.

A more apparent distinction according to two different trends is emphasized by $FeO + Fe_2O_3/FeO + Fe_2O_3 + MgO$ vs. SiO_2 plots (fig. 15). Both trends are characterized by a noticeable iron enrichment, which is not typical for calc-alkaline rocks ranging between SiO_2 50 % and 60 %. The upper trend shows a pattern which parallels the experimental curve obtained on liquids fractionally crystallizing under constant pO_2 of 10^{-7} atm in the system $MgO\text{-}FeO\text{-}Fe_2O_3\text{-}CaAl_2Si_2O_8\text{-}SiO_2$ (HAMILTON and ANDERSON, 1967). The lower trend, distinct but similar to the first, is characterized by an even steeper slope in the section between SiO_2 55 % and 58 %.

3.3. TRACE AND RE ELEMENTS

Trace element distribution of Alicudi samples is reported in Table 2.

Residual trace elements (Ba, Rb and Zr) show a linear positive correlation with La + Ce, used as a fractionation index, in the diagram of fig. 16. Total abundances of Rb and Zr are in the range suggested for most calc-alkaline to high-K calc-alkaline associations (TAYLOR, 1969; JAKES and WHITE, 1972). Ba concentration (300 to 700 ppm) is distinctly higher than the average given by TAYLOR (1969) and JAKES and WHITE (1972) for island arcs, but similar abundances have been observed in some high-K calc-alkaline rock suites (e.g. Eastern Papua, by JAKES and SMITH, 1970). The K/Rb ratio mostly ranges between 300 and 400 (fig. 17 *a*) and tends to decrease with increasing differentiation, following a pattern usually ascribed to fractional crystallization (JAKES and WHITE, 1970).

Strontium (600-700 ppm) is slightly higher than the average composition reported

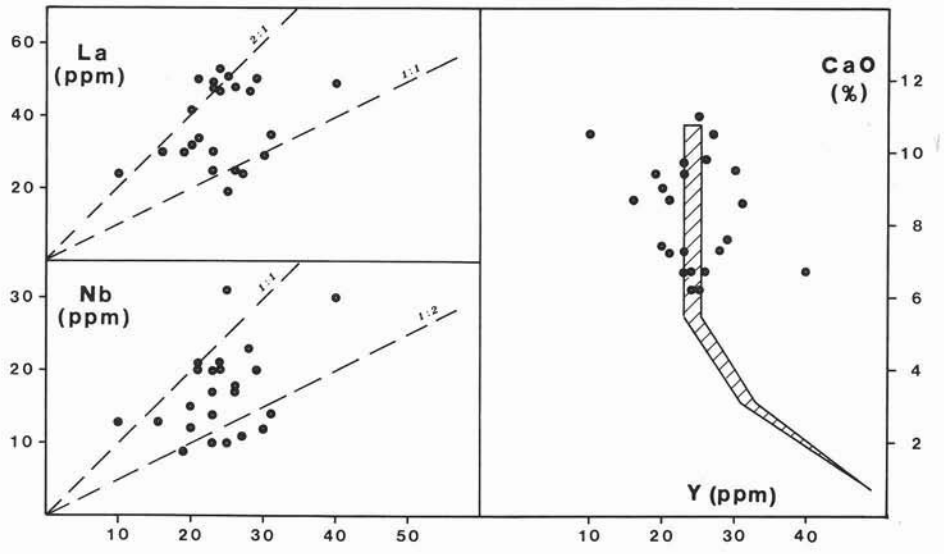

Fig. 19. — Island of Alicudi. La, Nb and CaO vs. Y plots for the Alicudi volcanics. La/Y and Nb/Y ratios show a high variability, but an overall increase of both ratios is noticed with increasing K_2O. The CaO vs. Y plot,where the standard calc-alkaline trend of LAMBERT and HOLLAND (1974) is reported (shaded area), shows an overall coherence of the Alicudi suite with the orogenic associations.

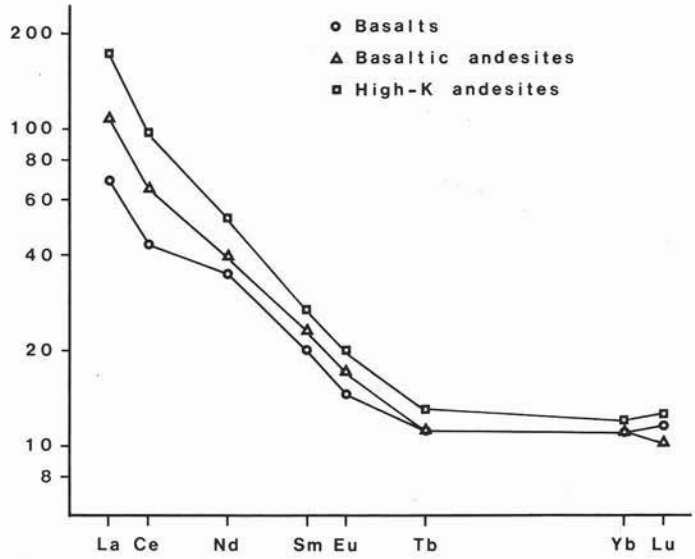

Fig. 20. — Island of Alicudi. REE distribution, normalized to chondritic abundance, is characterized by a strongly enriched LREE pattern. Minor variations in HREE are observed through the rock suite, while LREE noticeably increase from basalts to high-K andesites.

by TAYLOR (1969) for calc-alkaline and high-K calc-alkaline rocks, but values like those observed at Alicudi are commonly found for high-K calc-alkaline suites (JAKES and SMITH, 1970; JAKES and WHITE, 1972). Sr increases as fractionation

proceeds (fig. 17 *b*), suggesting that feldspars are not a major early-crystallizing phase.

Ferromagnesian trace elements (Cr, Ni and V) are characterized by unusually high concentration in most of the basalts and basaltic andesites, and they decrease with increasing La + Ce content (fig. 18).

It is however to be stressed that two different trends are clearly defined (Cr and Ni), showing a similar pattern. High Ni and Cr in SiO_2-poor calc-alkaline rocks is usually considered to result from olivine and clinopyroxene accumulation, but this

TABLE 3

REE analyses of Alicudi volcanics (Aeolian Islands) *

	Al 13	Al 02	Al 23	Al 010	Al 16
La	21 ± 1	34 ± 1	31 ± 1	46 ± 2	57 ± 2
Ce	36 ± 2	56 ± 4	53 ± 3	78 ± 5	86 ± 6
Nd	20 ± 1	25 ± 2	20 ± 1	27 ± 2	34 ± 2
Sm	4.2 ± .2	5.6 ± .2	3.9 ± .1	4.9 ± .2	6.4 ± .2
Eu	1.07 ± .04	1.29 ± .05	1.16 ± .04	1.3 ± .05	1.51 ± .05
Tb	.55 ± .07	.62 ± .08	.46 ± .06	.55 ± .07	.74 ± .09
Yb	2.2 ± .2	2.6 ± .2	1.9 ± .1	2.2 ± .2	2.6 ± .2
Lu	.36 ± .06	.32 ± .05	.30 ± .05	.36 ± .06	.47 ± .08

* INAA by A. PECCERILLO, University of Florence (Italy).

is not the case for Alicudi volcanics, where samples belonging to different trends show the same mode. The distinction of the two trends correlates with the characteristics previously emphasized as far as the $FeO + Fe_2O_3/FeO + Fe_2O_3 + + MgO$ ratio is concerned: samples belonging to the low-Cr and low-Ni trend show higher values of the ratio but a less marked iron enrichment pattern (upper trend of fig. 19).

The Nb and Y concentration is highly variable and the Nb/Y ratio ranges from 0.4 to 1.3. A similar variability is also observed for the La/Y ratio (fig. 19). In spite of such a scattered distribution, an overall increase of La/Y and Nb/Y ratios is observed with increasing K_2O content.

The CaO vs. Y plot (fig. 19), where the standard calc-alkaline trend of LAMBERT and HOLLAND (1974) is reported, show that the evolution of the Alicudi suite is coherent with the behavior of the orogenic associations.

REE concentration is reported in Table 3 and pattern in fig. 20 is characterized by strongly enriched LREE. Minor variations in HREE are observed through the rock suite, while LREE noticeably increase from basalts to high-K andesites. The La/Yb ratio ranges from 9.5 to 22.0, showing a positive linear correlation with K_2O. The high La/Yb ratio of high-K andesites is a character typically found for

K-rich orogenic rocks in island arc environments (JAKES and JILL, 1970).

$Sr^{87/86}$ analyses of Alicudi samples show values of 0.7040 (KLERKX et al., 1974) and 0.7055 (BARBERI et al., 1974).

4. - Conclusion

The island of Alicudi is the summit part of a huge strato-volcano, widely extending below sea level. Four subsequent volcanic cycles have been recognized on the island, giving rise to the piling up of lavas flows, endogenous domes and pyroclastic layers. Lava flows prevail among products of the first cycle, while pyroclastics dominate the second cycle. The third and fourth cycles mainly consist of lava flows and domes.

No stratigraphic evidence exists about the age of the volcanism concerned. The absence of Quaternary raised beaches, which are observed on some of the islands of the Aeolian Archipelago (Filicudi, Salina, Panarea and Lipari), may account for the recent age of the island or, alternatively, any trace of existent raised beaches may have been cancelled by sea erosion.

The volcanic activity on the island maintained a central character through time. No parasitic vents have been observed and the exposed feeding systems show a radial pattern relative to the main axis of the strato-cone. A large caldera formed at the end of the first cycle of activity and was later filled by the products of the second cycle. A volcanic depression (crater or caldera?) developed at the top of the second cycle volcanic pile and was partially filled and obscured by the endogenous domes and viscous lava flows of the latest volcanic activity.

Volcanic products range in composition from basalts to high-K andesites and are characterized by a fast rise of K_2O during differentiation. Major and trace element chemistry, coherently with the mineralogy of the lavas, points to a magmatic affinity which is transitional between calc-alkaline and high-K calc-alkaline.

The potassium-type trace elements (Rb, Sr and Ba) show high concentration, which is typical for the Aeolian volcanism (KELLER, 1974) and frequently reported with reference to island arc settings where high-K calc-alkaline to shoshonitic products occur (JAKES and SMITH, 1970; JAKES and WHITE, 1972).

A peculiar feature of the Alicudi rock suite is the high Ni and Cr abundance in most of the basalts and basaltic andesites. Concentrations up to 300 ppm (Cr) and 100 ppm (Ni) are observed on the basaltic end members of the association. Two distinct trend showing a similar pattern can be traced on both the diagrams Ni vs. La + Ce and Cr vs. La + Ce (fig. 18). The anomalous high Cr and Ni concentration observed in some high-K calc-alkaline series from Eastern Papua has been interpreted as the result of partial melting of a source material probably containing a mica phase (JAKES and SMITH, 1970). The same explanation does not hold for the Alicudi volcanics because of the lack of any apparent distinction on Rb and Ba plots (fig. 16), which would be expected to match the sharp difference observed on Cr and Ni distribution. A further element against a partial melting

model involving a mica phase is the alternate occurrence of low- and high-(Cr, Ni), rocks in the stratigraphic sequence. Peculiar features of the source material may be suggested to account for magma generation on a regional scale, but they do not apply to variations observed on a given volcanic structure.

It is speculatively suggested therefore that both trends may proceed from a common, more basic parent and differentiation occurred under different physico-chemical conditions, accounting for a sharp variability of Cr and Ni partitioning between liquidus and fractionating solidus.

Some petrographic features, e.g. the lack of Fe-Ti oxides amoung phenocrysts in basalts and basaltic andesites, and chemical characters as suggested by $FeO + Fe_2O_3/FeO + Fe_2O_3 + MgO$ vs. SiO_2 plots (fig. 15), point to fractionation having occurred under relatively low pO_2 conditions. It should be stressed as well that the investigated rock series is dominated by the early crystallization of ferro-magnesian phases relative to plagioclase, suggesting that the fractionation may have been controlled by high pH_2O, at least in the range basalt - basaltic andesite.

It is concluded, therefore, that the Alicudi orogenic rock suite results from fractionation processes acting, at variance with the neighboring island of Filicudi (VILLARI, this volume), under low pO_2 and high pH_2O.

The high concentration of K_2O, LREE and LILE, which is typical for the Aeolian Island magmatism, suggests that different degrees of partial melting may have affected a common source region giving rise to parent magmas further evolving under different conditions. Both melting and differentiation may account for the observed inter-island variations.

The cognate characters shown by the Aeolian volcanic products are in agreement with the evolution of the arc dynamics as suggested by BARBERI et al. (1973, 1974) and may reflect a relatively fractionated mantle source (KELLER, 1974) and/or a contribution of relevant elements from the subducted slab (RINGWOOD, 1974; NICHOLLS, 1974).

Appendix

SAMPLE CAPTIONS

GALERA VOLCANIC COMPLEX

Al 13 - Lava boulder from a volcanic agglomerate at the base of the cliff near Sc. Galera, western coast of the island.

Al 11 - Lava flow at the base of the volcanic pile outcropping along the cliff to the South of Sc. Galera, western coast of the island.

Al 25 - Lava flow from the volcanic sequence outcropping along the sea-cliff, northern coast of the island.

Al 24 - Lava flow from the base of the same volcanic pile as sample Al 25, northern coast of the island.

Al 23 - Dike cutting the volcanic sequence along the northern coast of the island.

DIRITUSO VOLCANIC COMPLEX

Al 27 - Lava flow at the base of the north-eastern slope, between Bazzina and Chierica.

Al 04 - Lava flow at the base of the volcanic pile filling the caldera, immediately above the angular unconformity along the south-western slope of the volcano.

Al 02 - Lava flow at the top of the volcanic pile filling the caldera along the south-western slope of the volcano.

Al 03 - Lava flow from the volcanic pile filling the caldera along the south-western slope of the volcano.

Al 22 - Lava flow from the northern upper slope of the volcano.

Al 06 - Lava flow from the northern rim of the crater, near Dirituso.

MONTAGNA VOLCANIC COMPLEX

Al 07 - Viscous lava flow from the upper south-western slope.

Al 011 - Viscous lava flow from the upper sout-eastern slope, near Pianicello.

Al 1 - Viscous lava flow from the lower south-eastern slope, near Tonna.

Al 09 - Viscous lava flow from the south-eastern slope.

Al 012 - Viscous lava flow from the eastern upper slope, near Montagna.

Al 08 - Viscous lava flow from the upper south-western slope, immediately above the flow unit from which sample Al 07 was collected.

Al 4 - Viscous lava flow at the base of the cliff, along the southern coast.

Al 01 - Endogenous dome on the south-western upper slope of the volcano.

Al 18 - Endogenous dome on the eastern upper slope of the volcano, near Montagna.

FILO DELL'ARPA COMPLEX

Al 010 - Endogenous dome from the summit area, at Filo dell'Arpa.

Al 013 - Endogenous dome of Filo dell'Arpa.

ISTITUTO INTERNAZIONALE DI VULCANOLOGIA - C.N.R.

CARTA GEOLOGICA DELL' ISOLA DI ALICUDI (ISOLE EOLIE)

GEOLOGICAL MAP OF THE ISLAND OF ALICUDI (AEOLIAN ISLANDS)

L. VILLARI - G. NAPPI (1975)

SCALA 1:10.000

0 500 1000m

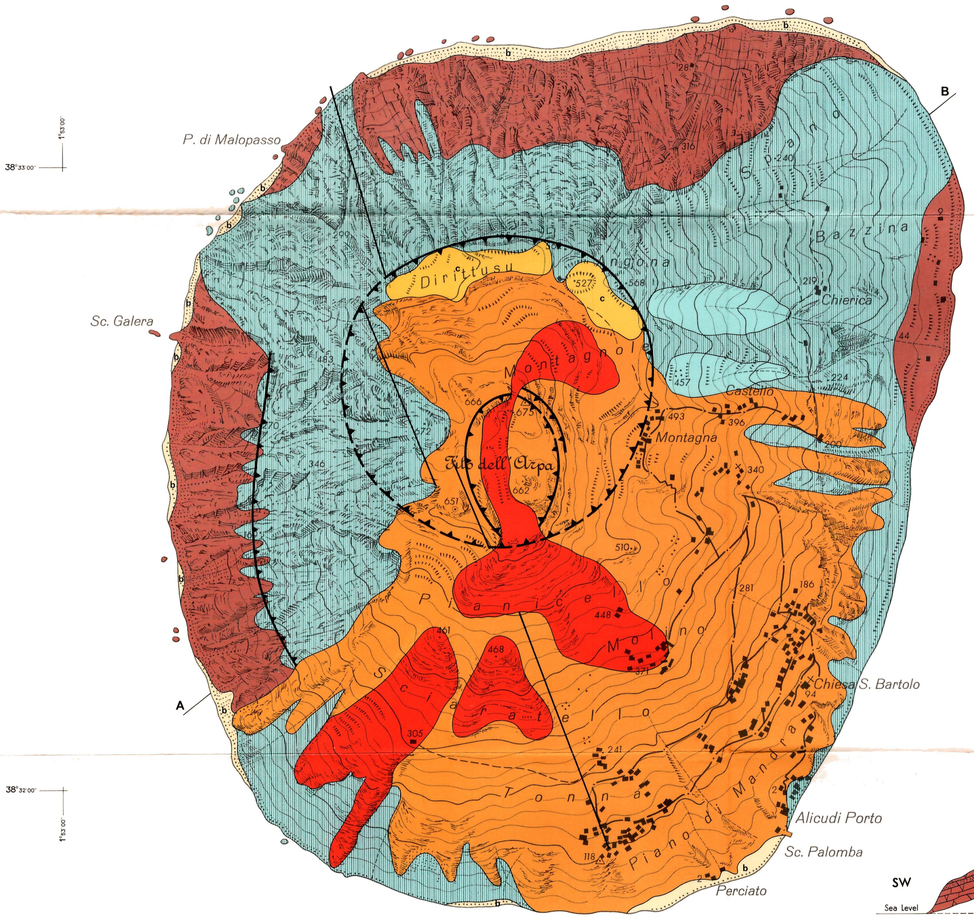

- Depositi vulcanoclastici rimaneggiati (c) e spiagge (b). Reworked volcanoclastic deposits (c) and beaches (b).
- Colate laviche viscose di Filo dell'Arpa (andesiti). Viscous andesite lava flows of Filo dell'Arpa.
- Colate laviche e cupole di Montagna (andesiti povere in silice e andesiti). Lava flows and domes of Montagna (low-Si andesites and andesites).
- Agglomerati vulcanici e breccie. Volcanic agglomerates and breccias.
- Colate laviche di Dirituso con subordinate intercalazioni di depositi piroclastici e scorie (basalti ricchi in allumina e andesiti). Lava flows of Dirituso with minor interbedded pyroclastic deposits and scoria (high-Al basalts and andesites).
- Colate laviche di Galera, densamente intersecate da dicchi e sills (basalti ricchi in allumina e andesiti povere in silice). Lava flows of Galera, densely cut by dikes and sills (high-Al basalts and low-Si andesites).
- Faglie. Faults.
- Orli di crateri e caldere. Craters and calderas rims.

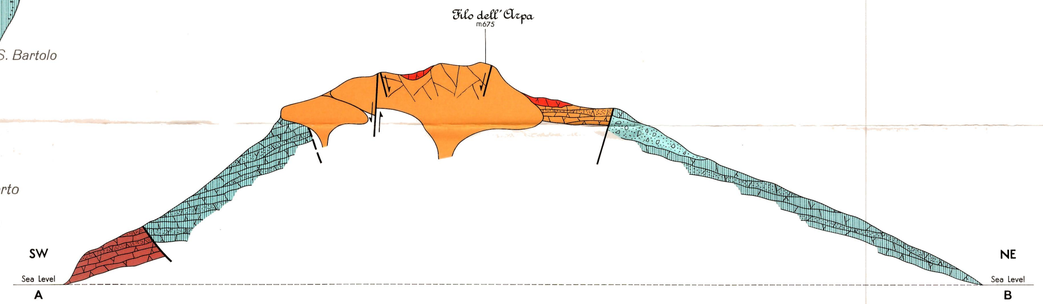

Litografia Artistica Cartografica - Via del Romito 11-13r. - Firenze 1977